Synthesis of Polydopamine-Like Nanocapsules via removal of a Sacrificial Mesoporous Silica Template with Water

Fabiana Nador,[a] Eduardo Guisasola,[b] Alejandro Baeza,[b] Miguel Angel Moreno Villaecija,[a] Maria Vallet-Regí,[b] Daniel Ruiz-Molina [a]*

Abstract: Hollow polymeric PDA micro-/nanocapsules have been obtained through a very simple, mild and straightforward method that involves coating of silica mesoporous nanoparticles through an ammonia-triggered polymerization of PDA and the posterior removal of the sacrificial template simply by dispersion in water, without the need of any harsh chemical reagent, either in the presence or absence of active principles, from doxorubicin to iron oxide nanoparticles. To demonstrate the potential of the nanocapsules obtained with this new approach, they have been successfully used as nanocarriers for drug delivery.

Hollow polymeric micro-/nanocapsules have attracted large interest due to their intrinsic characteristics such as low density, high surface-to-volume ratio or encapsulation. These features have made them attractive in many current and emerging areas of technology such as encapsulates, catalyst support and energy storage.[1] To fabricate these capsules, different chemical and physicochemical approaches have been used, including self-assembly of block copolymers, spray-drying and gas-blowing, among others.[2] Though, one of the approaches most successfully used is colloidal template synthesis.[3-6] In this method, a solid core is coated using a physical or chemical process such as layer-by-layer (LbL) or direct chemical deposition to provide an intermediate called the core–shell structure. The core particles are subsequently removed by selective dissolution in an appropriate solvent or by calcination at an elevated temperature in air to produce hollow capsules.

Oxidative self-polymerization of dopamine (DA) on surfaces, inspired by the adhesive properties displayed by mussels, has been previously employed to generate a range of polydopamine (PDA) core–shell structures.[7-10] Thus, capsules made of PDA by removal of the sacrificial template core would combine the most significant features of facile, rapid and controllable self-polymerization from DA with the tunable sacrificial template synthesis. Several solid templates to obtain PDA capsules have been so far reported, among them polystyrene solid beads (PS),[11,12] calcium carbonate ($CaCO_3$) particles[13,14] and more widely silica nanoparticles (mainly non-porous). Specifically in this last case, different successful examples of PDA nanocapsules obtained upon removal of silicon-based core have been developed.[2,7,15-17] In all these cases HF solutions were needed to dissolve the silicon core hampering most of the times the use of mesoporous silica nanoparticles with encapsulated materials.[18]

Herein we report a new facile approach for the in situ fabrication of PDA capsules from silica mesoporous nanoparticles (MSNs) making use of a new ammonia-triggered catechol polymerization recently reported by our group.[19,20] This new polymer is not only able to coat individual MSNs through a generalized single-step synthesis but also allows for the posterior removal of the sacrificial template simply by dispersion in water or a buffer solution, without the need of any harsh chemical reagent, thereby avoiding the limitations so far found especially if sensitive chemical materials are to be encapsulated (see Figure 1). This fact has allowed for the in-situ fabrication of a variety of new biocompatible PDA-like capsules loaded with different cargos, including iron oxide nanoparticles (an inorganic material), the doxorubicin drug (Dox) and a combination of them. Moreover, the nanocapsules not only encapsulate but also allow for the controlled release of the encapsulated Dox at different pH values favouring their use as vehicles for drug delivery systems as demonstrated with Human Osteosarcoma cells (HOS).

In a typical experiment, dopamine was dissolved in isopropanol and polymerized with an aqueous solution of ammonia (25% in water) at 45 ºC. Simultaneously, MSNs prepared according to a modified Stöber method (see Experimental Section and Supporting Information, S1),[21] were added resulting in the formation of well defined, uniform and reproducible coatings after 12 h. Moreover, in order to examine the role of the particle size in the coating process, two different batches of MSNs were prepared. From now on MSN_{140} or MSN_{350} refer to MSN nanoparticles used in this work with a mean size of 140 nm or 350 nm, respectively.

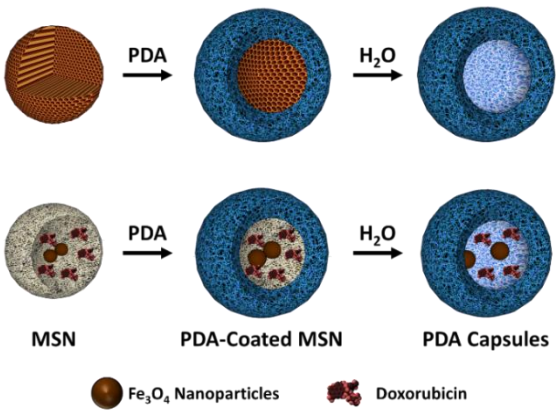

Figure 1. Schematic representation of the PDA-coating formation around MSN particle, followed by self-removal process triggered by water, leading to the formation of the hollow PDA nanocapsules

[a] Dr. F. Nador, M. A. Moreno Villaecija, Dr. D. Ruiz-Molina
Catalan Institute of Nanoscience and Nanotechnology (ICN2), CSIC and The Barcelona Institute of Science and Technology,
Edificio ICN2, Campus UAB, Bellaterra, 08193 Barcelona, Spain
E-mail: dani.ruiz@icn2.cat:

[b] E. Guisasola, Dr. A. Baeza, Prof. M. Vallet-Regí
Depto. Química Inorgánica y Bioinorgánica. Instituto de Investigación Sanitaria Hospital 12 de Octubre i+12 Universidad Complutense de Madrid. Plaza Ramon y Cajal s/n.
Centro de Investigación Biomédica en Red de Bioingeniería, Biomateriales y Nanomedicina (CIBER-BBN), Av. Monforte de Lemos, 3-5. Pabellón 11. Planta 0 28029 Madrid, Spain.

Supporting Information is available from the Wiley Online Library or from the author: experimental details, FT-IR, XRD, STEM, SEM, EDX, DLS, thermogravimetric analysis, linear isotherm adsorption and BJH pore size distribution (PDF). STEM video (avi).

First family of nanoparticles to be studied was MSN_{140}. STEM images shown in Figure 2b confirmed the formation of a consistent coating around the silica core. An EDX scan profile along the line drawn across the diameter of typical PDA-coated MSN_{140} (MSN_{140}@PDA) showed carbon signal on the most external coating, whereas a silicon signal was detected only in the core of MSNs. This result was in agreement with a MSN core-shell structure with a diameter ranging between 100-140 nm surrounded by a PDA polymer shell with an average thickness of 40 nm. FT-IR also revealed PDA-coating on MSNs particles with bands in the range of between 1615-1485 cm^{-1}, attributed to the stretching C-C of the benzene rings and the bending N-H of the PDA.[22] Stretching bands at 1084 cm^{-1} and 948 cm^{-1} corresponding to asymmetric and symmetric modes of Si-O-Si bond, respectively, were also found (see Figure S6). Dynamic light scattering (DLS) of $MSNs_{140}$ and MSN_{140}@PDA showed average diameters of 180 ± 40 nm and 330 ± 50 nm, respectively (see Figure S7). The coating induced a diameter increase due to the PDA coating itself (80 nm) and some residual agglomeration though no significant aggregation was detected (see Experimental Section).

Strikingly, when the MSN_{140}@PDA nanoparticles were exposed to water or a PBS buffer (pH~7.4 or pH~5) at 37ºC for 24–48 h, monodisperse nanocapsules were obtained upon self-removal of the silica core as shown in Figure 2c. It is important to remark that the removal of the MSN takes place only for the washing step and not along the coating process. Exposure of non-coated MSNs to the same water or PBS buffer solutions at different pHs did not result in any effect over the silica material in the same time period (see Figure S8).

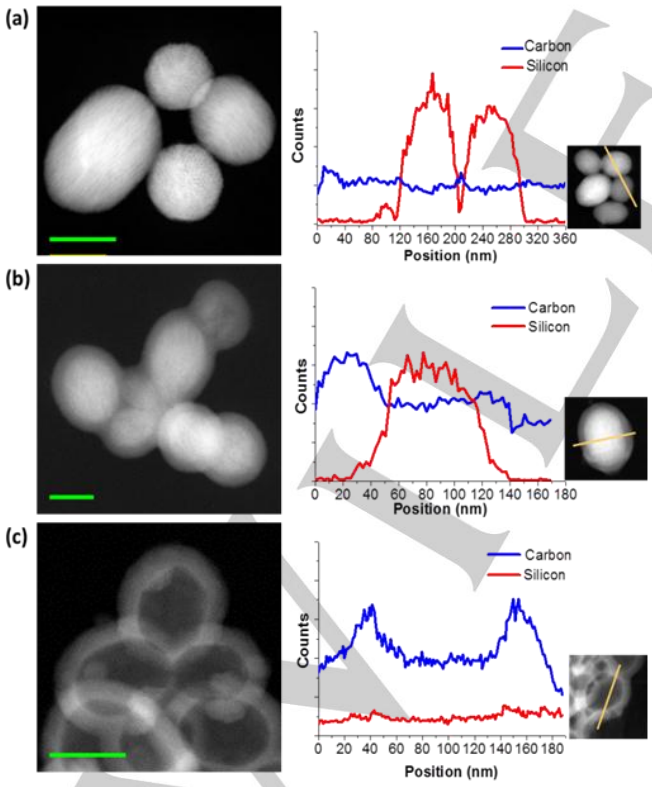

Figure 2. STEM images and EDX line scan profiles along the line drawn across the diameter of (a) MSN nanoparticles, (b) PDA-coated MSNs and (c) PDA nanocapsules. Aggregation of the nanoparticles occurs upon drying of the sample. Scale bars are 100 nm.

To prove that two experiments were done. Firstly, 10 mg of MSNs were dispersed in 13 mL of i-PrOH and then 25% NH_3 in H_2O (10 mmol, 0.75 mL) was added (without dopamine). The sample was heated at 45°C and it was left during 12 h under magnetic stirring. The final MSNs were separated in two fractions B01 and B02: B01 was washed three times with EtOH while B02 remained unwashed (see Figure S8). Finally, both B01 and B02 (5 mg) were placed in a flask containing 100 mL of H_2O. The samples were left during 48 h under magnetic stirring at 37°C. The final pH was neutral in both cases. STEM images shown in Figure S10 revealed that the structure of the MSNs remains intact after H_2O exposition for both B01 and B02 confirming that there is no effect of the NH_3 on the final dissolution of the nanoparticles. Indeed, even in the case of B02 where no washing was done and therefore NH_3 would have remained inside the pores, no effect was found. The second experiment consisted of exposure of non-coated MSNs to water or PBS buffer solutions at different pHs. However, any effect over the silica material was detected. This result is in agreement with previously reported works which indicate that the MSNs dissolution in PBS required around one week or even more in the case of polymer coated MSN.[23,24]

STEM images of solid samples revealed that nanocapsules retained their empty interior and aggregation phenomena after drying. EDX line scan profiles also proved the existence of a polymeric carbon shell with an average coating thickness of 40 nm, similar to that found prior to silica removal, with no significant trace of silicon within the PDA nanocapsules (see Figure 2c and Supporting Information, S3). Moreover, FT-IR of the capsules dialyzed against PBS during 48 h showed only a strong band in the range between 1690-1485 cm^{-1} corresponding to PDA (see Figure S9).

Similar results were obtained for MSN_{350}@PDA nanoparticles; exposure to water or PBS buffers also resulted in the formation of PDA nanocapsules (see Figure S10 and S11), without any typical FT-IR bands related to MSNs. The main difference between both families of capsules lies at the time needed to completely remove the silica core. Indeed, exposure of the MSN_{140}@PDA nanoparticles to water or PBS buffer for less than 24 hours resulted in the partial removal of the sacrificial silica template (see Figure S12), whereas for MSN_{350}@PDA core-shell nanoparticles shorter exposure times were needed (down to only seven hours in some cases), for the complete removal of the MSN core (data not shown). Zeta potential values remained quite homogenous around -30/-40 mV along the series MSN_{350}, MSN_{350}@PDA and PDA capsules (see Figure 3a). Such values were negative enough as to ensure a good dispersion of the particles. The negative potential values for the MSNs are expected to arise from surface silanol groups and not significant change was observed after PDA coating. This is in accordance with the presence of catechol moieties in the outer surface of the PDA shell and later capsules. In this way, DLS measurements of the nanocapsules revealed a distribution of diameters centered on 600 nm (with a tail heading to higher diameters). Considering that the average diameter of PDA capsules observed by STEM images was 400/450 nm (see Figure 3b), a good dispersion in solution is obtained (with a small deviation arising mainly from swelling of the nanoparticles, some minor aggregation phenomena or a combination of them). Worth to mention, once the nanocapsules are dried for their characterization they exhibit the typical tendency of polymeric nanoparticles to aggregate as shown in Figure 3.

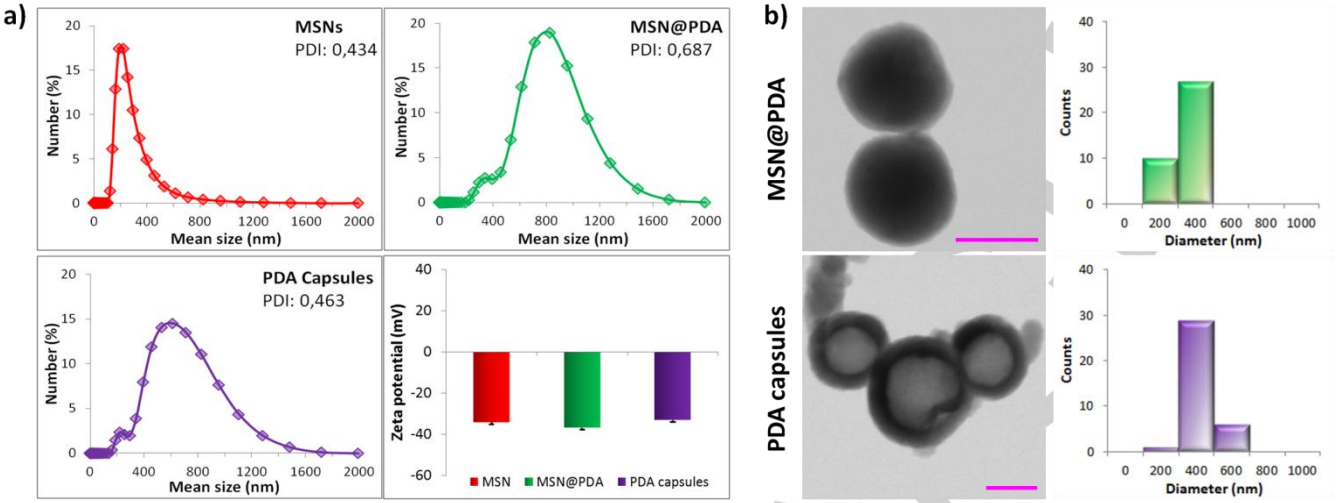

Figure 3. (a) DLS and Zeta potential measurements for $MSNs_{350}$ (♦), MSN_{350}@PDA (♦) and PDA capsules (♦) in PBS (pH~7, 0.002M). (b) STEM images and histogram with size distribution for MSN_{350}@PDA particles and PDA capsules. Aggregation of the nanoparticles occurs upon drying of the sample. Scale bars are 200 nm.

Additional experiments to check the stability of the PDA nanocapsules on different solvents were performed (see Figure S13). The results indicated that the PDA capsules were quite stable in organic solvents like THF, dichloromethane or alcohols, or in aqueous solutions in a wide range of pHs (2-12). However, in solvents like DMF or toluene some degradation of the capsules could be detected.

Worth to mention, the formation of the PDA coating was only effective when the polymerization reaction is carried out with ammonia; no proper coating was found when the polymerization reaction takes place with tris buffer neither $NaIO_4$.Similar results were obtained for an imine-based bis-catechol, for which a proper coating is obtained only upon polymerization with ammonia. Moreover, the polymerization reaction and posterior coating was done with three new additional solvents (methanol, acetone and acetonitrile). Even though successful, more homogenous and monodisperse coatings were still obtained with isopropanol (see Supporting Information, S4). In some specific cases such is the case of acetone the coating did not work even.

Further experiments were done to understand the silica removal mechanisms. Tentatively, it was initially attributed to the formation of selective catechol-silica complexes with the general formula $[Si(C_6H_4O_2)_3]$ as previously reported by Mizutani et al.[25] This process was even highly favored in our case by the presence of the PDA coating rich in amines/polyamines groups, which have already been shown to increase the silica dissolution rates by 15-25 times.[26] To confirm this hypothesis, a new experiment was designed consisting in the replacement of dopamine by guaiaretic catechol without amine functional groups. Reaction of this new catechol with an aqueous ammonia solution in the presence of MSN nanoparticles resulted in the formation of the corresponding coating, as previously described for DA (see Figure S25). However, no nanocapsules were formed upon exposure of the hybrid core-shell nanoparticles to water or the PBS buffer for 48 h. Moreover, exposure of the MSN nanoparticles to a non-polymerized dopamine buffer solution did not affect either the integrity of the MSNs (see Figure S26). Therefore, only those amine-based groups resulting upon reaction of DA with ammonia seem to be effective on the silica removal. Lastly, the higher surface area and large pore network of the mesoporous MSN nanoparticles coated in this work,[27] were also expected to enhance the dissolution process rate as previously reported.[28] To confirm this, non-porous commercial silica nanoparticles (mean size around 20 nm) were coated with the target PDA polymer and exposed to water or PBS buffers for 72 h; after this time no significant changes were detected in the system (see Figure S27).

This findings supports that the silica dissolution mediated by catechols cannot be the only reason for the silica elimination, since the guaiaretic cathecol do not induce any SiO_2 elimination after the polymerization process. On the other hand, the DA is not able to dissolve silica by itself. Consequently, the silica elimination process must be governed by the species formed in the polymerization process. Polymerization of DA involves the formation of polyamines and other functional groups. Especially polyamines are known to play a role in control over the dissolution or precipitation of silica in some marine species.[29]

The simple methodology followed for the formation of the nanocapsules was used next to encapsulate different active materials. First, as a proof-of-concept, monofunctional Fe_3O_4@PDA nanocapsules, were obtained. For this first Fe_3O_4@MSN nanoparticles (for the complete characterization see Supporting Information, S6) were coated with PDA resulting in the formation of a Fe_3O_4@MSN@PDA core-shell intermediate. Afterwards, exposure to water or a PBS buffer resulted in the formation of PDA capsules containing Fe_3O_4 (see Supporting Information, S7). FT-IR of the Fe_3O_4@PDA nanocapsules showed in this case a small peak around 1084 cm^{-1} from remaining silica (see Figure S35), which most likely remained due to interactions with the iron oxide nanoparticles.[30,31] The presence of iron oxide inside the PDA nanocapsules (and not just simply deposited underneath) was checked by carrying out

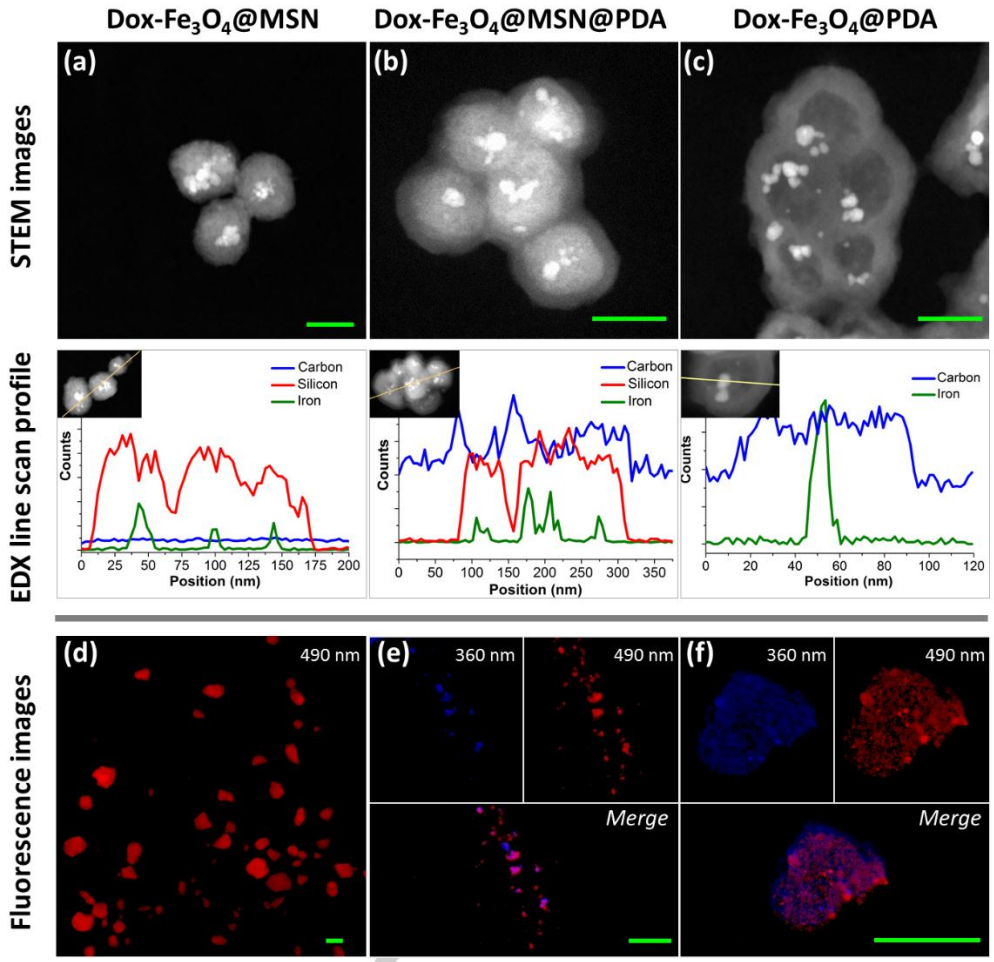

Figure 4. (a-c) STEM images and EDX line scan profiles of Dox-Fe_3O_4@MSN_{50}, Dox-Fe_3O_4@MSN_{50}@PDA and Dox-Fe_3O_4@PDA. Scale bars are 50 nm. (d-f) Fluorescence microscope images of Dox-Fe_3O_4@MSN_{50}, Dox-Fe_3O_4@MSN_{50}@PDA and Dox-Fe_3O_4@PDA to the excitation wavelength thereby indicated. Scale bars are 20 μm.

a tomographic reconstruction from STEM by rotation of the sample from -60 to +60 degrees (see video and Figure S36). Similar successful encapsulation results were obtained for the drug containing nanoparticles Dox@MSN (for synthetic and characterization details see Experimental Section and Supporting Information, S8). The presence of encapsulated Dox in the final Dox@PDA nanoparticles was detected by optical fluorescence in red region after excitation at λ:490 nm. A low intensity of blue autofluorescence from PDA was also detected in this case after excitation at λ:360 nm (see Figure S37 and S38).[32,33] The lower transmission of the core (less contrast with the PDA polymeric shell) of Dox@PDA by comparison with empty PDA nanocapsules also points out to the presence of encapsulated Dox (see Figure S39).[34] Finally, treatment of Dox@PDA nanocapsules in DMF at 80ºC during 2 hours induced a progressive degradation of the container and therefore, the release of encapsulated drug showing that the amount of loaded doxorubicin was approximately 2.4 % (w/w) as determined by fluorescence spectroscopy.

Simultaneous encapsulation of Dox and Fe_3O_4 nanoparticles was also attempted (for synthetic details see Experimental Section in the Supporting Information). Beyond encapsulation of several biomaterials have been carried out simultaneously through LbL assembly by direct coating of the target or loading into preformed LbL-assembled capsules,[7,15,35-36] time-consuming and intensive assembly protocol has been considerably reduced through the presented procedure.

Combined STEM micrographs and fluorescence microscope images of the three steps, Dox-Fe_3O_4@MSN, Dox-Fe_3O_4-@MSN@PDA and Dox-Fe_3O_4@PDA, are shown in Figure 4. As can be seen there, STEM images revealed in this case the formation of MSNs 50 nm average width with embedded iron oxide nanoparticles (average diameters of 10 nm), clearly distinguished due to their different electronic density (Figure 4a top). Moreover, EDX line scan profile along the sample confirmed the presence of Si and Fe elements (Figure 4a bottom). The presence of additional doxorubicin in Dox-Fe_3O_4@MSN_{50} was detected by optical fluorescence in red region after excitation at λ:490 nm (Figure 4d). In a second step, Dox-Fe_3O_4@MSN_{50} was coated by PDA films with an average thickness of 20 nm (Figure 4b top). A considerable increase in the carbon proportion was detected by an EDX line scan profile regarding uncoated Dox-Fe_3O_4@MSN_{50} particles (Figure 4b bottom). The same figure also confirmed the presence of the encapsulated iron oxide in addition to the red fluorescence provided by doxorubicin (see Figure 4e). Dox-Fe_3O_4@MSN_{50}@PDA diameters of 300 ± 50 nm were obtained by DLS measurements (see Figure S29), most likely due to some minor aggregation phenomena induced by the presence of the iron oxide nanoparticles (as previously described, larger aggregation takes place after drying). On the last step,

bifunctional Dox-Fe_3O_4@MSN_{50}@PDA nanoparticles were exposed to the core removal conditions already described above resulting in the formation of hollow PDA nanocapsules encapsulating iron oxide nanoparticles (see Figure 4c) and doxorubicin, as confirmed by fluorescence (see Figure 4f).

EDX element mapping of C, Fe and Si performed for Dox-Fe_3O_4@PDA on the area drawn revealed mostly the presence of iron inside the nanocapsule whereas the shell was mainly formed by carbon. Furthermore, silicon element mapping confirmed the presence of some traces of this element in the interior of the Dox-Fe_3O_4@PDA nanocapsule shell as well as in the core around iron oxide (see Figure S41).

Prior to this work, PDA encapsulation was only possible through a systematic study of the permeation of small molecules through the PDA shell, with a posterior cargo release strongly dependent on the PDA coating thickness,[37] the concentration gradient and the mass transfer resistance through coating.[38] Likewise, Ji et al. carried out silica microcapsules formation through self-template dissolution–regrowth mechanism and subsequent drug loading by immersion process, tuning the shell pore diameters at different pHs.[39] Taking into consideration the works mentioned above, the green synthetic approach for the PDA nanocapsules formation reported in this article is therefore of special relevance for the encapsulation of sensitive chemical materials under mild conditions and in a single synthetic step.

As a proof-of-concept to demonstrate such potential, we have used the Dox@PDA nanocapsules for drug delivery. With this aim, accumulative controlled release studies of Dox were carried out by exposing the Dox@PDA nanocapsules to pH 5, 7 and 9 buffer solutions through a Corning® Transwell® permeable support, withdrawing the supernatant every time step. The use of different pHs is remarkable as long as the differential electrostatic interactions between the cargo and the zwitterionic PDA polymeric coating allow to control the release.[12] Figure 5a reveals a 9 % drug release at pH 9 within the first 24 h while only 1.4 % and 2 % of Dox release are observed for pH 5 and 7 respectively. A second experiment (Figure 5b) shows that the leaked Dox at pH 5 during the first 48 h is greatly hindered. The Dox release was then triggered by changing the sample to pH 9 buffer, reveling a 12 % (3.7 μg·mL^{-1}) drug release in only 24 h more. This fact supports that the PDA nanocapsules possess a solid sustained Dox release profile and strong pH dependency similar to those already described in the literature which confirms the validity of our approach.[37]

Finally, Human Osteosarcoma cells (HOS) were exposed to different concentrations of PDA and Dox@PDA capsules for 24 hours. The cytotoxicity was evaluated by flow cytometry using Annexin V/propidium iodide protocol for cell death determination. Cell statically studies showed that the samples exposed to empty capsules up to 100 μg·mL^{-1} presented a good survival ratio confirming the absence of toxicity of the PDA capsules (see Figure 5c). In order to evaluate the capacity of these capsules to deliver therapeutic agents to diseased cells, different concentration of Dox@PDA nanocapsules were added to HOS cell cultures and their viability were evaluated after 24 hours; the released Dox was enough to provoke significant cell viability reduction of 25% at doses of 100 μg·mL^{-1} (see Figure 5d). This result combined with the fact that PDA capsules present even higher drug release profiles at mild-basic conditions could be useful for the development of drug-loaded nanocarriers suitable for the treatment of tumors characterized by basic environments as colon,[40,41] or after induction of metabolic alkalosis by intraperitoneal administration of $NaHCO_3$.[42]

In summary, we have reported a new experimental approach for the formation of hollow PDA capsules via self-removal of a sacrificial mesoporous silica template simply upon exposure to water, thanks to the use of a novel ammonia-triggered PDA polymer. Although there are previous reports on the formation of catechol-based hollow capsules via colloidal templating synthesis, this is the first time that this is done under such mild conditions, allowing for the encapsulation of different active species including inorganic nanoparticles. As a proof-of-concept to demonstrate the potential of this approach, we have evaluated the capacity of these novel nanocapsules as carries to deliver Dox, with a significant cell viability reduction whereas empty PDA nanocapsules did not reveal any cell toxicity.

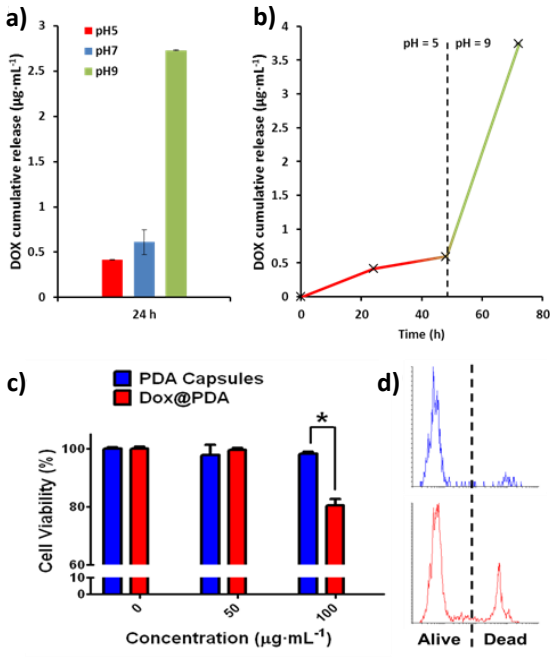

Figure 5. Cumulative doxorubicin release from Dox@PDA nanocapsules: (a) 24 h Dox release at three different pHs and (b) the Dox release over time with pH 9 trigger at 48 h. (c) Cell viability of HOS cells treated with PDA and DOX@PDA capsules. *p < 0.05 (Student's t-test). (d) Alive vs death ratio of cells exposed at 100 μg·mL^{-1} of PDA (blue line) and DOX@PDA (red line), respectively.

Acknowledgements

F. N. thanks Universidad Nacional del Sur for supporting her postdoctoral stay. E.G. thanks CEI Campus Moncloa for the PICATA fellowship. ICN2 acknowledges support from the Severo Ochoa Program (MINECO, Grant SEV-2013-0295). This work was supported by the project MAT2015-70615-R and MAT2012-35556 from the Spanish Government, CSO2010-11384-E (Agening Network of Excellence) and FEDER funds. We thank A. C. Hudson for editorial revision.

Keywords: catechol, encapsulation, polydopamine, mesoporous, nanocapsules

[1] X. W. Lou, L. A. Archer, Z. Yang, *Adv. Mater.* **2008**, *20*, 3987.
[2] G. L. Li, H. Mohwald, D. G. Shchukin, *Chem. Soc. Rev.* **2013**, *42*, 3628.
[3] Y. Wang, A. S. Angelatos, F. Caruso, *Chem. Mater.* **2008**, *20*, 848.
[4] G. L. Li, H. Möhwalda, D. G. Shchukinab, *Chem. Soc. Rev.* **2013**, *42*, 3628.
[5] V. Malgras, Q. Ji, Y. Kamachi, T. Mori, F.-K. Shieh, K. C.-W. Wu, K. Ariga, Y. Yamauchi, *Bull. Chem. Soc. Jpn.* **2015**, *88*, 1171.
[6] Y. Zhang, B. Y. W. Hsu, C. Ren, X. Li, J. Wang, *Chem. Soc. Rev.* **2015**, *44*, 315.
[7] A. Postma, Y. Yan, Y. Wang, A. N. Zelikin, E. Tjipto, F. Caruso, *Chem. Mater.* **2009**, *21*, 3042.
[8] S. Kang, M. Baginska, S. R. White, N. R. Sottos, *ACS Appl. Mater. Interfaces* **2015**, *7*, 10952.

[9] J. Zhou, P. Wang, Ch. Wang, Y. T. Goh, Z. Fang, P. B. Messersmith, H. Duan, *ACS Nano* **2015**, *9*, 6951.
[10] B. J. Kim, T. Park, H. C. Moon, S.-Y. Park, D. Hong, E. H. Ko, J. Y. Kim, J. W. Hong, S. W. Han, Y.-G. Kim, I. S. Choi, *Angew. Chem. Int. Ed.* **2014**, *53*, 14443.
[11] F.-F. Cheng, J.-J. Zhang, F. Xu, L.-H. Hu, E. S. Abdel-Halim, J.-J. Zhu, *J. Biomed. Nanotechnol.* **2013**, *9*, 1155.
[12] Q. Liu, B. Yu, W. Ye, F. Zhou, *Macromol. Biosci.* **2011**, *11*, 1227.
[13] L. Zhang, J. Shi, Z. Jiang, Y. Jiang, S. Qiao, J. Li, R. Wang, R. Meng, Y. Zhua, Y. Zhenga, *Green Chem.* **2011**, *13*, 300.
[14] X. Chen, Y. Yan, M. Müllner, M. P. van Koeverden, K. Fung Noi, W. Zhu, F. Caruso, *Langmuir* **2014**, *30*, 2921.
[15] C. J. Ochs, T. Hong, G. K. Such, J. Cui, A. Postma, F. Caruso, *Chem. Mater.* **2011**, *23*, 3141.
[16] Y. Wang, V. Bansal, A. N. Zelikin, F. Caruso, *Nano Lett.* **2008**, *8*, 1741.
[17] Q. Zheng, T. Lin, H. Wu, L. Guo, P. Ye, Y. Hao, Q. Guo, J. Jiang, F. Fu, G. Chen, *Int. J. Pharm.* **2014**, *463*, 22.
[18] H. C. Genuino, N. N. Opembe, E. C. Njagi, S. McClain, S. L. Suib, *J. Ind. Eng. Chem.* **2012**, *18*, 1529.
[19] J. Saiz-Poseu, J. Sedó, B. García, C. Benaiges, T. Parella, R. Alibés, J. Hernando, F. Busqué, D. Ruiz-Molina, *Adv. Mater.* **2013**, *25*, 2066.
[20] B. García, J. Saiz-Poseu, R. Gras-Charles, J. Hernando, R. Alibés, F. Novio, J. Sedó, F. Busqué, D. Ruiz-Molina, *ACS Appl. Mater. Interfaces* **2014**, *6*, 17616.
[21] A. Baeza, E. Guisasola, A. Torres-Pardo, J. M. González-Calbet, G. J. Melen, M. Ramirez, M. Vallet-Regí, *Adv. Funct. Mater.*, **2014**, 24, 4625.
[22] M. Sureshkumar, C.-K. Lee, *Carbohydr. Polym.* **2011**, *84*, 775.
[23] H. Yamada, Ch. Urata,Y. Aoyama, S. Osada, Y. Yamauchi, K. Kuroda, *Chem. Mater.*, **2012**, *24*, 1462.
[24] V. Cauda, Ch. Argyo, T. Bein, *J. Mater. Chem.* **2010**, *20*, 8693.
[25] T. Mizutani, K. Takahashi, T, Kato, J. Yamamoto, N. Ueda, R. Nakashima, *Bull. Chem. Soc. Jpn.* **1993**, *66*, 3802.
[26] S. V. Patwardhan, G. E. Tilburey, C. C. Perry, *Langmuir* **2011**, *27*, 15135.
[27] Q. He, J. Shi, M.Zhu, Y. Chen, F. Chen, *Microporous and Mesoporous Materials*, **2010**, *1–3*, 314.
[28] X. Zheng, J. Zhang, J. Wang, X. Qi, J. M. Rosenholm, K. Cai, *J. Phys. Chem. C*, **2015**, *119*, 24512.
[29] N. Poulsen, M. Sumper, N. Kroger, *Proc. Natl. Acad. Sci.* **2003**, *100*, 12075.
[30] Y. Xu, L. Axe, *J. Colloid Interface Sci.* **2005**, *282*, 11.
[31] A. Scheidegger, M. Borkovec, H. Sticher, *Geoderma* **1993**, *58*, 43.
[32] A. Yildirim, M. Bayindir, *Anal. Chem.* **2014**, *86*, 5508.
[33] C, Zhao, F, Zuo, Z. Liao, Z. Qin, S. Du, Z. Zhao, *Macromol. Rapid Commun.* **2015**, *36*, 909.
[34] Y. Gao, X. Wu, L. Zhou, Y. Su, C.-M. Dong, *Macromol. Rapid Commun.* **2015**, *36*, 916.
[35] A. Yu, Y. Wang, E. Barlow, F. Caruso, *Adv. Mater.* **2005**, *17*, 1737.
[36] D. G. Shchukin, A. A. Patel, G. B. Sukhorukov, Y. M. Lvov, *J. Am. Chem. Soc.* **2004**, *126*, 3374.
[37] B. Yu, D. A. Wang, Q. Ye, F. Zhou, W. Liu, *Chem. Commun.* **2009**, 6789.
[38] B. Yu, J. Liu, S. Liu, F. Zhou, *Chem. Commun.* **2010**, *46*, 5900.
[39] Q. Ji, C. Guo, X. Yu, C. J. Ochs, J. P. Hill, F. Caruso, H. Nakazawa, K. Ariga, *Small* **2012**, *8*, 2345.
[40] K. Sonaje, K.-J. Lin, S.-P. Wey, C.-K. Lin, T.-H. Yeh, H.-N. Nguyen, C.-W. Hsu; T.-C. Yen, J.-H. Juang, H.-W. Sung, *Biomaterials* **2010**, *31*, 6849.
[41] N. Rouge, P. Buri, E. Doelker, *Int. J. Pharm.* **1996**, *136*, 117.
[42] N. Raghunand, B. Mahoney, R. van Sluis, B. Baggett, R. J. Gillies, *Neoplasia* **2001**, *3*, 227.

COMMUNICATION

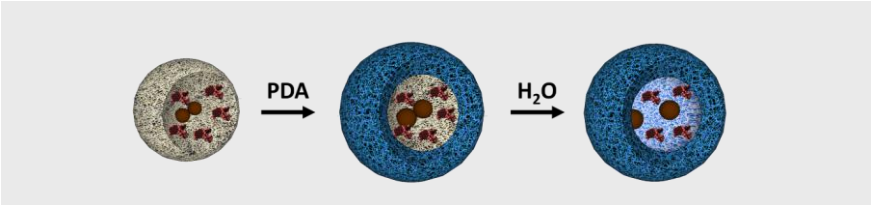

Hollow PDA capsules are obtained through a very simple and straightforward approach based on the formation of hybrid mesoporous silica-PDA nanoparticles and subsequent self-removal of the inorganic core with water. This mild approach together with the encapsulation abilities of MSN nanoparticles allow for the encapsulation of different active principles, from inorganic nanoparticles to drugs or a combination of them in a straight manner. Finally, to demonstrate the potential of this new approach, the novel nanocapsules have been successfully used as drug delivery carriers on Human Osteosarcoma cells.

*F. Nador, E. Guisasola, A. Baeza, M. A. Moreno Villaecija, M. Vallet-Regí, D. Ruiz-Molina **

Page No. – Page No.

Synthesis of Polydopamine-Like Nanocapsules via removal of a Sacrificial Mesoporous Silica Template with Water